ELSEVIER

Journal of Alloys and Compounds 293–295 (1999) 364–368

Journal of ALLOYS AND COMPOUNDS

A duplicated fluorination technique for hydrogen storage alloys

Y.-M. Sun*, X.-P. Gao, N. Araya, E. Higuchi, S. Suda

Department of Environmental and Chemical Engineering, Kogakuin University, Nakano-machi 2665-1, Hachioji-shi, Tokyo, 192-0015, Japan

Abstract

The fluorination technique developed in 1991 has been experimentally confirmed to be effective for modifying alloy surfaces to extremely high activation characteristics and a highly protective nature against poisoning materials such as air, water vapour, and carbon oxides in gas–solid reaction. However, the dissolution of a considerable amount of Ni during the fluorination process has been left as an unsolved problem for further development. The aim of this work is to prevent the decrease of the Ni concentration on the treated surface. A fluorination technique named as the duplicated fluorination technique, presented here aims at enriching the metallic Ni onto the increased surface area of the alloy by varying the pH-value down and up repeatedly in a definite range. Experimental studies have been performed extensively on the duplicated fluorination of $LaNi_{4.7}Al_{0.3}$ and $LmNi_5$ based alloy particles. The surface reaction characteristics were found to be greatly improved as the results of (1) the removal of oxides, (2) its high affinity to both ionic and molecular hydrogen, and (3) its high electron conductivity of the functionally-graded surface composed of the enriched Ni and fluoride layer. The microstructure, element distribution, and composition analysis were examined by using scanning electron microscopy (SEM), electron probe microanalysis (EPMA) and inductively coupled plasma spectrometry (ICPS).

Keywords: Duplicated fluorination; Spherical metallic Ni; Specific surface area

1. Introduction

The fluorination technique (F-1 treatment) has been developed as one of the sophisticated techniques for improving the surface properties and electrochemical performances of hydrogen storage alloy electrodes [1–3]. The complicated surface structure and cracks generated by the formation of fluoride and hydride on the particle surfaces during the fluorination process result in an increase of the specific surface area by several tens of times compared to the untreated one [4]. Therefore, further investigation for generating much larger specific surface area and higher surface activity through an improved fluorination process is required in order to improve the initial activation characteristics and the electrochemical durability of electrode during charging/discharging cycles [5,6].

Various fluorination techniques such as F-1, F-2, F-3, F-4, F-5 and others [7], have been developed and used for different applications according to their special advantages [8–12]. The fluorination technique (F-4 treatment) has been developed for increasing the specific surface area [13]. The aim of this work is to develop a more advanced fluorination technique, which includes an elimination of the oxide layer from the alloy surface, an increase of the specific surface area and an improvement of the surface activity and durability of alloy particles.

The $LaNi_{4.7}Al_{0.3}$ alloy powder for the gas–solid reaction and LmNi-based alloy powder for electrode materials were treated by duplicated fluorination. The microstructure, elemental distribution and composition analysis were examined by SEM, EPMA and ICPS. The effects of the fluorinated alloys on the initial activation characteristics and electrochemical performance were discussed.

2. Experimental details

$LaNi_{4.7}Al_{0.3}$ (gas–solid reaction) and $LmNi_5$-based (electrochemical reaction) alloys were ground mechanically to fine powder of about 35 μm in size. The powder then was fluorinated in an aqueous solution containing F^- and Ni^{2+} ions at a controlled pH range (6.0–7.0) by repeatedly applying a buffer solution (named process A). After 30 min, a reducing agent $NaH_2PO_2 \cdot H_2O$, was added into the fluorination system to continue the treatment (named process B). The fluorinated alloy powders were rinsed several times with distilled water and dried in vacuum.

*Corresponding author.

0925-8388/99/$ – see front matter
PII: S0925-8388(99)00403-X

The surface distribution of constituent elements was measured by EPMA. The BET method was also employed to determine the specific surface area.

The initial activation in gas–solid reaction was performed at 40°C for both the fluorinated and unfluorinated samples by using the Sieverts apparatus as described earlier [14]. The following electrochemical experimental conditions were established: charging 200 mA/g for 3 h, discharging at 150 mA/g to −0.6 V vs. Hg/HgO reference electrode after resting for 10 min at 20°C.

3. Results and discussion

3.1. pH-value change of the fluorination process

It is important to make the pH-value vary down and up repeatedly between 6.0 and 7.0 during the duplicated fluorination process [13]. The variation of the pH-value in these processes (A and B) is shown in Fig. 1. In process A, the pH-value was controlled by using CH_3COONa–CH_3COOH buffer solution for increasing the specific surface area. In process B, Ni^{2+} ions were reduced to metallic Ni by adding the reducing agent $NaH_2PO_2 \cdot H_2O$.

3.2. Effects of the treatment time

3.2.1. Specific surface area as a function of the treatment time

The specific surface area as a function of the treatment time for the process B is shown in Fig. 2. The specific surface area was significantly increased by controlling the pH and the time in the process A [13]. By extending the treatment time of process B, the specific surface area decreased slightly. The decrease of the specific surface area is caused by the growth of metallic Ni, which covered the fluoride layer with a fine network structure formed in process A. The amount of deposited Ni on the particle surface can be controlled by changing the treatment time in process B. For every treatment the specific surface area of the sample after fluorination was much larger than that of the untreated one.

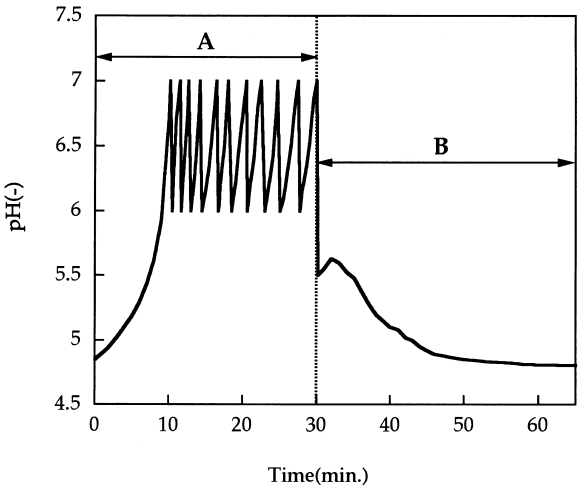

Fig. 1. Curve of pH-change controlled during the duplicated fluorination.

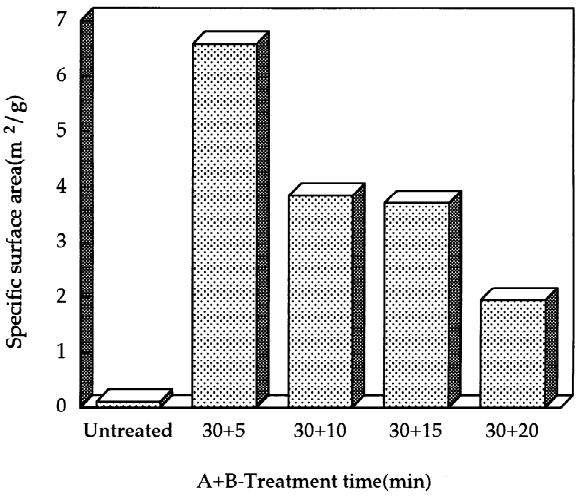

Fig. 2. The change of specific surface area of particles after the duplicated fluorination.

3.2.2. Amount of Ni reduced as a function of the treatment time

In the case of application of the duplicated fluorination procedure on AB_5 alloy, the Ni-concentration in process A and process B was different. The concentration of Ni^{2+} ion in the F-solution in process A increased due to the dissolution of NiO formed on the surface, however, the concentration of Ni^{2+} ion in the F-solution in process B decreased significantly due to the reduction and deposition of Ni on the particle surface. In addition, the pH value changes in process B became slower with increasing treatment time as can be seen in Fig. 1 due to the decrease of sites where Ni could be deposited. Therefore, the surface modification should be carefully optimized by controlling fluorination time and the fluorination speed in both process A and B.

3.3. Morphology of fluorinated particles surface

3.3.1. Surface morphology

The surface morphology of the unfluorinated and fluorinated alloy particles for varied treatment conditions was observed by SEM (Fig. 3). The unfluorinated particle surface showed an extremely smooth surface (Fig. 3(a)), however the fluorinated surface was formed with a rather complex structure. In particular, very fine spherical crystals of about 1.0 μm were obtained by increasing the treatment time in process B. Furthermore, Fig. 3(d) showed a significant change of the content and size of spherical particles with increasing treatment time in process B. Assuming spherical particles to be uniform, the amount of

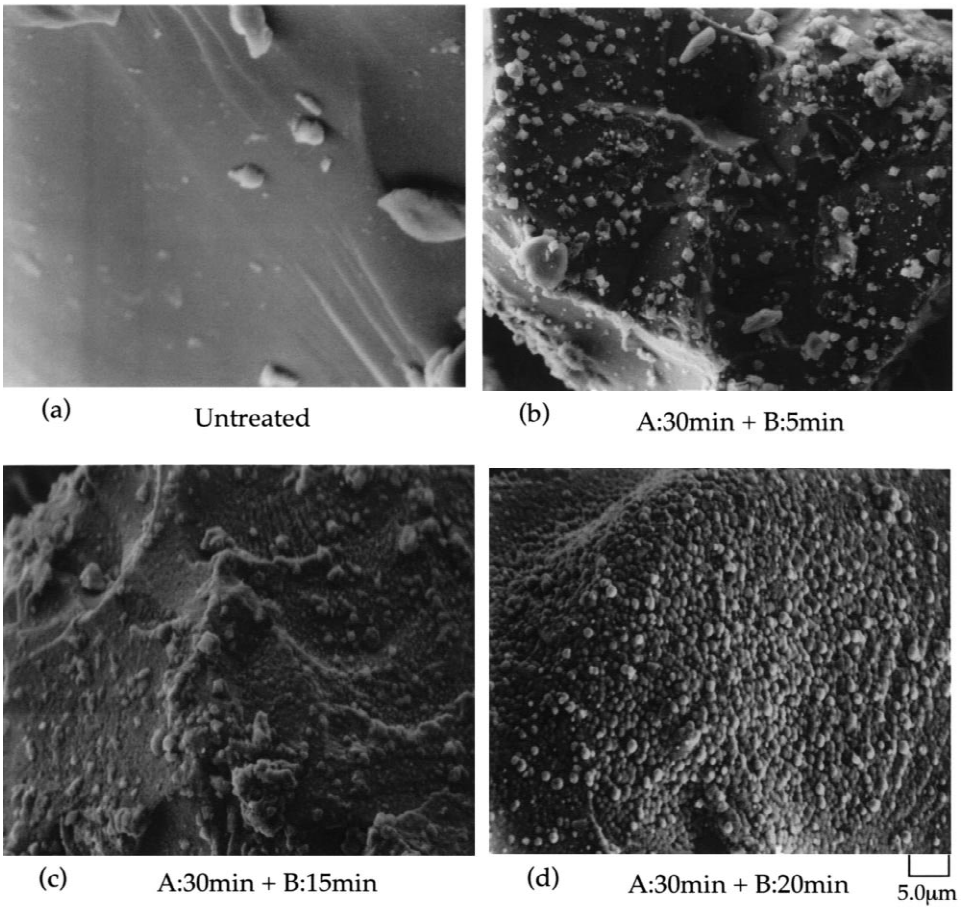

Fig. 3. The surface morphology of the fluorinated and unfluorinated particles.

the spherical particles per unit area was increased by eight times during a reaction period of 15 min. The special surface structure formed by the spherical Ni particles and the fluoride layer was considered to play an important role for the hydrogen uptake process.

3.3.2. Section observation of fluorinated particles

The section observation and the element distribution of the fluorinated particles taken by SEM and EPMA were illustrated in Fig. 4. It was found from these images of the fluorinated particles that many cracks of the order of submicrometers were observed toward the centre of particles. From those results, the hydrogenation reaction was found to proceed during the fluorination process. It was believed that the hydrogenation reaction during the fluorination was influenced by the expansion of lattice interstices, and by the increase of the specific surface area which contributed considerably to the initial activation characteristics of hydrogen storage alloys. It was easily found from the section mapping of F that F invaded the inside of cracks and the fluoride layer covered the surface during the fluorination.

The state of reduced Ni was further identified by using EPMA analysis of the section mapping of Ni. The metallic Ni dispersed at particle surface can be found after a long time fluorination as shown in Fig. 3, which was in agreement with the above mentioned result by SEM.

3.4. Effect of the fluorination on the hydriding reaction

The initial activation in the gas–solid reaction for the fluorinated $LaNi_{4.7}Al_{0.3}$ alloy and unfluorinated one was given in Fig. 5. For the untreated alloy, the incubation period for the initial hydrogen absorption was more than 20 min. After fluorination, the initial activation characteristics were significantly improved as shown in above figure. The reaction rate increased further with increasing time of process B due to the increased Ni amount reduced and deposited at the particle surface. Metallic spherical Ni at the particle surface contributed to the improvement of the initial activation in gas–solid reaction.

3.5. The electrochemical characteristics

Fig. 6 showed the electrochemical characteristics of electrodes before and after fluorination. For the short treatment time in process A, the electrode exhibited a

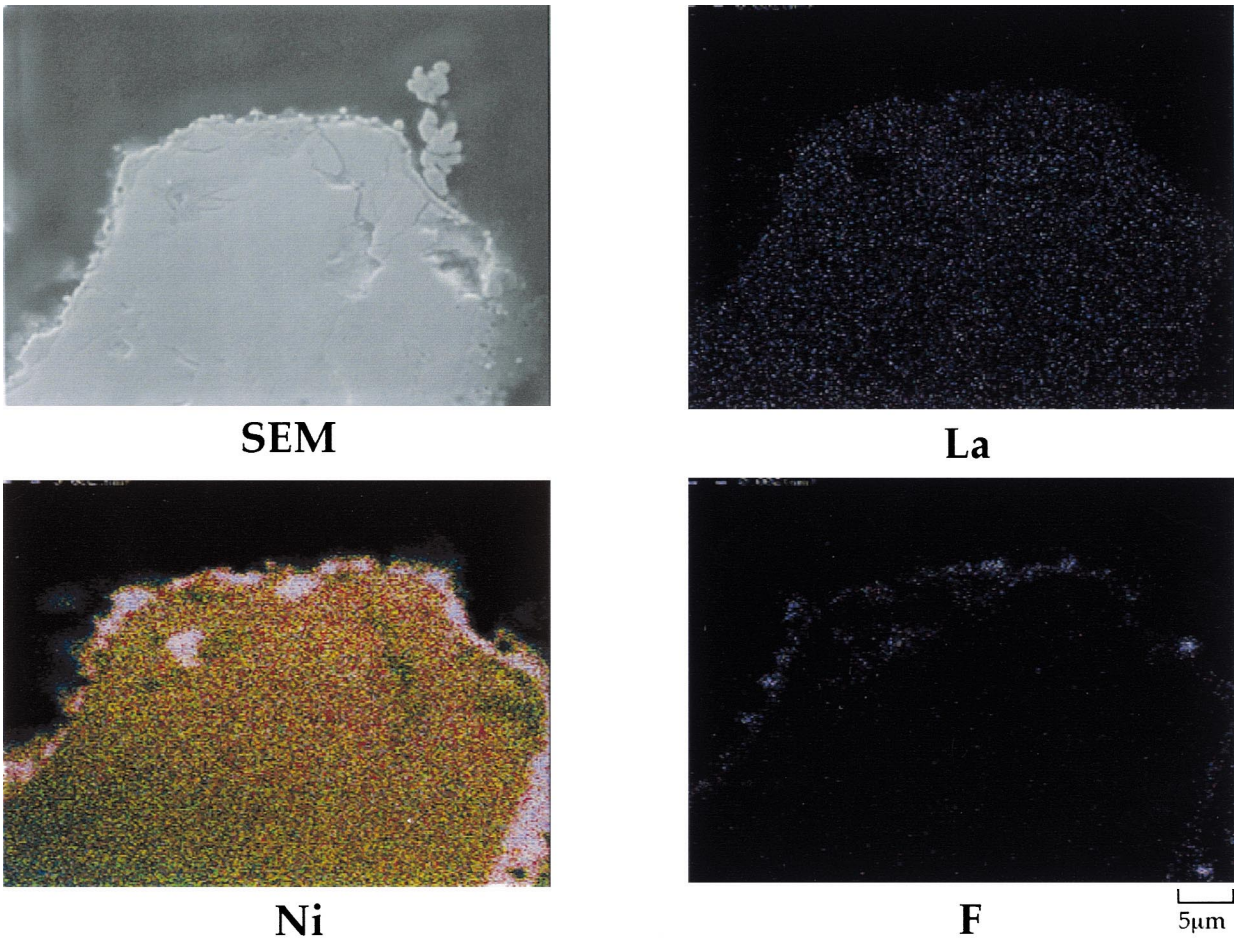

Fig. 4. The sectional SEM image and element distribution of the duplicated fluorinated particle.

higher maximum capacity and a better initial activation as compared to the untreated electrode due to both the formation of fluoride and the reduction of metallic Ni at the particle surface. On the other hand, the cycle life of the fluorinated electrode was significantly improved especially over 300 cycles for the long treatment time in process A due to the formation of a thick fluoride layer. Therefore, the formation of the fluoride layer on the particle surface

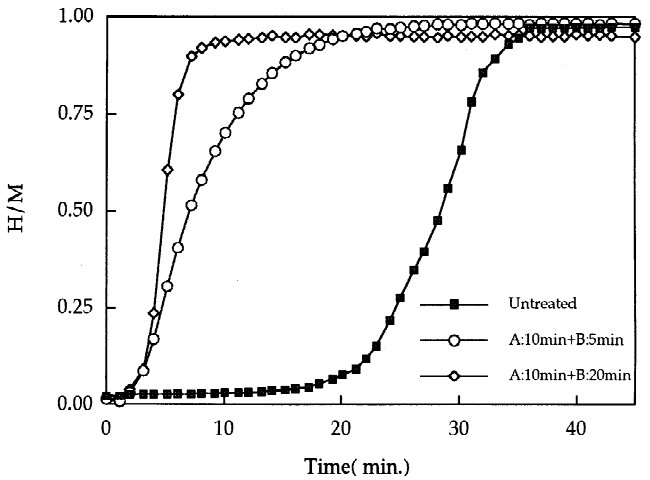

Fig. 5. The initial activation in gas–solid reaction for the fluorinated and unfluorinated alloy.

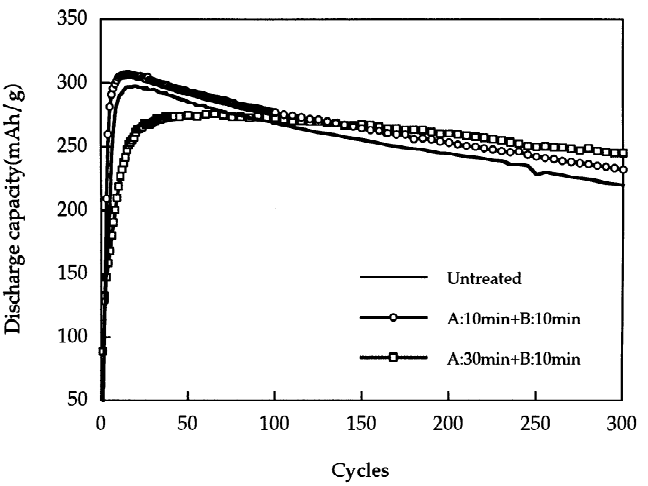

Fig. 6. The initial activation and cycle life of the fluorinated and unfluorinated alloy.

added to the durability of the electrode although the maximum capacity was decreased slightly to some extent.

4. Conclusion

The spherical metallic Ni was formed and deposited at the particle surface with an increased specific surface area by applying the new fluorination technique consisting of two processes. The specific surface structure formed during the treatment resulted in a significant improvement of the initial hydrogen uptake in the gas–solid reaction by extending the treatment time in process B. The electrochemical cycle life was improved by increasing treatment time in process A due to the formation of fluoride at the particle surface. The main effects of the duplicated fluorination were: (1) the removal of oxides, (2) the high affinity to hydrogen, (3) the excellent hydrogen uptake rate and (4) a good durability of electrode during cycling of the functionally-graded surface composed of the enriched spherical Ni and fluoride layer.

References

[1] Y.-M. Sun, K. Iwata, S. Chiba, Y. Matsuyama, S. Suda, J. Alloys Comp. 253–254 (1997) 502–524.
[2] E. Hikuchi, M. Sakashita, Zh.-P. Li, S. Suda, Res. Rep. Kogakuin Univ. 83 (1997) 27–30.
[3] A. Okutsu, M. Sakashita, Zh.-P. Li, S. Suda, Res. Rep. Kogakuin Univ. 83 (1997) 23–26.
[4] Y.-M. Sun, S. Chiba, S. Suda, Res. Rep. Kogakuin Univ. 82 (1997) 78–81.
[5] S. Suda, G. Sandrock, Phys. Chemie 183 (1994) S149–S156.
[6] S. Suda, Res. Rep. Kogakuin Univ. 83 (1997) 13–18.
[7] S. Suda, Zh.-P. Li, Y.-M. Sun, MRS 98, Spring Meeting Program & Registration Materials, H7.7 (1998) 154.
[8] S. Suda, Res. Rep. Kogakuin Univ. 78 (1993) 29–34.
[9] Y.-M. Sun, S. Suda, J. Alloys Comp. 231 (1995) 417–421.
[10] F.-J. Liu, G. Sandrock, S. Suda, J. Alloys Comp. 190 (1992) 57.
[11] X.-L. Wang, S. Suda, J. Alloys Comp. 194 (1992) 73–76.
[12] F.-J. Liu, S. Suda, Res. Rep. Kogakuin Univ. 78 (1995) 95–104.
[13] Y.M. Sun, S. Okamoto, N. Araya, S. Suda, Res. Rep. Kogakuin Univ. 84 (1998) 51–54.
[14] F.-J. Liu, M. Ito, S. Suda, Res. Rep. Kogakuin Univ. 72 (1992) 85–89.